Robotic Swing-up Regrasping Manipulation based on Impulse-Momentum approach and cLQR control

Avishai Sintov, *Student Member, IEEE,* Or Tslil and Amir Shapiro, *Member, IEEE*

***Abstract*—In this paper we present the swing-up regrasping problem where an object is manipulated using a robotic arm around a point pinched by the arm's gripper. The aim of the regrasping is to manipulate the object from an initial angle to regrasp it on a new desired angle relative to the gripper. The pinching point functions as a semi-active joint where the gripper is able to apply only frictional torques on the object to resist its motion. We address the problem by proposing a novel approach. The approach incorporates an impulse-momentum method with an LQR-based controller for stabilization on the desired angle. In particular, a sub-optimal Clipped LQR controller is presented to deal with the dissipative semi-active joint. The interaction of these methods with the unique property of the semi-active joint is investigated and analyzed. Simulations on a six degrees of freedom manipulator regrasping a bottle validate the proposed approach. Moreover, a full experiment was conducted on a robotic arm to test the approach and the control of a semi-active joint. The simulations and experiment have proven the feasibility of the method.**

***Index Terms*—Regrasping, robotic manipulations, swing-up, Clipped LQR.**

I. Introduction

The use of the same end-effector to grasp an object in various orientations performing different tasks dramatically increases its capabilities. This can be achieved by alternating grasp configurations of the object with respect to the task to be done and is known as *Regrasping* [1]. The ability of robots to perform regrasping tasks enhances their capabilities and dexterity. For instance, in assembly lines, the same arm can perform multiple operations on the same part and by that decrease the number of robotic arms in the plant. However, for efficiency, the regrasping should be done fast. Therefore, dynamic regrasping is preferred utilizing the arm's dynamics, gravity, and inertia to manipulate the object in the gripper. Our long-term goal is to build a library of basic dynamic regrasping manipulations that will serve as building blocks for higher task executions. In this paper we address a part of the dynamic regrasping problem termed *Swing-up Regrasping*. Swing-up regrasping motions are usually performed by human hands to alter the angle between the palm and a grasped object (Figure 1). This is a dynamic manipulation to grant the object enough energy to reach the desired angle while rotating around a pivot point between the pinching fingers. Gravity and friction can assist the swing-up manipulation. The fingers vary the force they apply on the object to control the velocity and final pose through friction.

Fig. 1. Hand swing-up regrasping of a marker from (a) initial angle to (c) final angle.

Current regrasping methodologies work only with highly redundant (and hence expensive) hand architectures, and require agile sensory feedback. In the robotics literature, there are three known approaches for regrasping. The first approach is picking and placing where the object is placed on a surface and picked up again in a different grasp configuration [2], [3]. The pick and place approach is rather slow and demands a large surface area around the robot. The second approach is the use of the end-effector's degrees of freedom to move between contact points while maintaining a force-closure grasp during the entire process. This approach is also called *quasi-static finger gaiting* in the robotics literature [4], [5], [6], [7], [8], [9]. However, quasi-static finger gaiting is quite wasteful, as it requires sufficiently many degrees of freedom (requiring highly redundant finger linkages) to manipulate the grasped object between two grasp configurations while maintaining force closure grasps. The third approach is much faster and efficient; however it is more complex, as it uses dynamical manipulations to switch between grasp configurations. The end-effector allows relative velocity with the object after releasing it through a series of dynamic manipulations and regains fixed contact by catching it at the final pose [10], [11]. Most work that utilize dynamic manipulations use a multi-fingered highly dexterous hand for performing regrasping. The work in [12] proposed a regrasping strategy based on visual feedback of the manipulated object, this with a multi-fingered hand. In [13] a regrasping method was introduced using a 3-finger hand with no external sensing for feedback.

In this paper we synthesize an approach for a robotic

A. Sintov, O.Tslil and A. Shapiro are with the Department of Mechanical Engineering, Ben-Gurion University of the Negev, Beer-Sheva 84105, Israel (Corresponding author: e-mail sintova@post.bgu.ac.il, phone +972-54-5562555).

arm to perform a swing-up regrasping from a lower energy angle to an higher one. The swing-up is done by accelerating the gripper pinching a pivot point on the object to increase its energy. It should be noted that unlike the human hand, a robotic arm can flip the object upside down and let the object free fall to the desired angle. This is analogous to flipping the human hand behind the back, which is of course not possible. We aim to mimic the swing-up motion of the human hand, which is limited by the shoulder. Our proposed approach for the swing-up regrasping problem is a gravity-assisted approach where the object is swung-up above the desired angle using an impulse-momentum method and then stabilized using a modified LQR controller.

The presented swing-up problem is partially inspired by the swing-up and stabilization control of a Pendubot [14] and an inverted pendulum [15] at the upright position. Energy control is widely used in such problems to stabilize the system's energy at a desired energy value [16], [17], [18]. This control method is used for swing-up to a region close enough to the desired state followed by a linear controller to balance on the desired state. Another approach for the swing-up is the impulse-momentum method [19], [20], where an initial impulse is applied to the system for a short period of time, which causes change of momentum and therefore transfer of energy.

An important matter discussed in this paper is the nature of the joint formed at the pinching (pivot) point. The gripper's jaws hold the object and enable relative velocity. Thus, torsional friction exists at the pivot and is controlled by the normal force of the jaws. Therefore, the pivot point is a joint that is able only to resist the motion of the object, i.e., can only dissipate energy. Such a joint is termed a *Semi-Active joint* and its notion arises from semi-active friction dampers [21], [22], [23]. By controlling the normal force, semi-active friction dampers greatly improve performance compared to passive dampers. Moreover, they consume a fraction of the power fully active dampers require. The common control method for semi-active friction dampers is the use of a Clipped Linear Quadratic Regulator (cLQR) [24], a version of which is applied in this work. We apply the notion of a semi-active joint and its control method to the robotic field. We model a semi-active robotic joint and control the swing-up and stabilization using these methods. This research not only proposes a novel approach but also investigates the composition of a semi-active joint with various control methods for the swing-up regrasping problem.

The paper is organized as follows. Section II defines the swing-up regrasping problem along with its mathematical models. The proposed approach is presented in Section III along with theoretical background. Simulations on a six degrees of freedom (DOF) robotic arm regrasping a bottle and a full experiment are presented in Section IV. Conclusions and future work are discussed in Section V.

II. Preliminaries

In this section we present the robotic arm model and object to be regrasped. The frictional interface model between the arm and object is presented along with the minimal normal force needed to prevent tangential slippage. Further, the problem definition is presented along with several assumptions. Finally, two conceptual solution approaches are introduced.

A. System model & dynamics

Consider an n-joint manipulator given by the dynamic equations of motion

$$D(\mathbf{q})\ddot{\mathbf{q}} + C(\mathbf{q}, \dot{\mathbf{q}})\dot{\mathbf{q}} + G(\mathbf{q}) = \mathbf{u_m}, \tag{1}$$

where $\mathbf{q}(t) = [\varphi_1(t) \cdots \varphi_n(t)]^T \in \mathbb{R}^n$ is the vector of joints' angles at time t, $\mathbf{u_m}(t) = [u_1(t) \cdots u_n(t)]^T \in \mathbb{R}^n$ is the torque control vector, D is an $n \times n$ inertia matrix, C is the $n \times n$ matrix of centrifugal and Coriolis acceleration terms, and G is an $n \times 1$ vector of generalized gravitational force. The world coordinate frame $\mathcal{O}$ is fixed at the base of the robotic arm. A simple jaw gripper is fixed at the tip of link n. Both jaws of the gripper are parallel such that they can apply parallel and equal forces $f_N \geq 0$ on a grasped object. The gripper's pitch angle is denoted by ψ and is measured relative to the vertical axis.

Given object $\mathcal{B}$ with mass m and length L held by the gripper at point e on the object termed the pivot point between the gripper and object. Let h be a plane containing the axis from link n's joint to point e and parallel to the gripper's jaws. Let the moment of inertia of $\mathcal{B}$ be I with respect to an object's Center of Mass (COM) on an axis perpendicular to h. Furthermore, let l be the distance from pivot e to the COM's projection on h. Angle θ is defined to be the angle between link n's axis and the axis formed by the COM and e. The swing-up problem is basically a planar problem. Therefore, the whole regrasping motion is performed in plane h and we assume that h is parallel to the gravity vector $\mathbf{g}$. Figure 2 is a planar example of such a system where h is the robot's motion plane.

Friction exists between the jaw gripper and the object at pivot point e. We assume a soft-finger contact model [25] between the jaw and object surfaces. In addition, for simplicity we denote both frictional torques exerted at each jaw as a single lumped equivalent torque τ, which of course equals their sum. When there is no relative velocity (i.e., $\dot{\theta} = 0$), the static friction torque τ_s exerted on pivot e is, according to the *Coulomb friction model*,

$$|\tau_s| \leq \gamma f_N \tag{2}$$

where $\gamma > 0$ is the static coefficient of torsional friction. When relative velocity exists, $\dot{\theta} \neq 0$, we use the *Signum-Friction Model* [26] expressing the friction torque as

$$\tau_m = -\nu f_N \text{sgn}(\dot{\theta}) \tag{3}$$

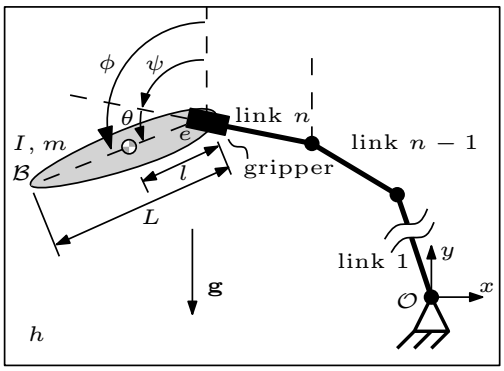

Fig. 2. Object gripped by the robotic arm with angle θ.

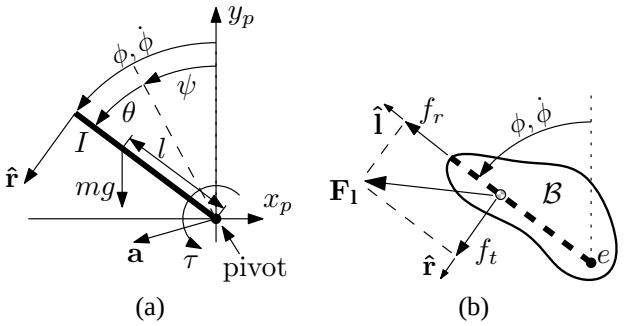

Fig. 3. (a) Object-Pendulum model and (b) Forces acting on the OPM.

where ν is the dynamic torsional coefficient of friction. Note that τ_m is a dissipative force and therefore has opposite direction to velocity. For changing velocities where the velocity crosses the $\dot{\theta} = 0$ line, switching between models (2) and (3) leads to numerical difficulties. Karnopp [27] proposed to define a small neighborhood of zero velocity, $|\dot{\theta}| \leq \varepsilon$ for some small $\varepsilon > 0$, where the friction torque τ is equal to the net torque τ_t acting on the object in order to preserve equilibrium. To maintain zero velocity, the normal force f_N will be chosen to counter-balance the net torque with $f_N = |\tau_t|/\gamma$. The overall friction model used in this work defines the friction torque τ with respect to the normal force as

$$\tau(f_N) = \begin{cases} -\gamma f_N \text{sgn}(\tau_t), & |\dot{\theta}| \leq \varepsilon \\ -\nu f_N \text{sgn}(\dot{\theta}), & |\dot{\theta}| > \varepsilon \end{cases} . \tag{4}$$

The presented model is an n-degrees robotic arm holding an object and enabling rotation around the holding pivot point. One may view this model as an under-actuated $(n+1)$-degrees of freedom arm with n actuated joints and one semi-actuated joint [22]. A semi-actuated joint enables only counter-acting the motion by controlling the normal force applied at the pivot point. That is, we apply a positive normal force while the outcome friction torque must satisfy the dissipative constraint

$$\tau \cdot \dot{\theta} < 0 \ . \tag{5}$$

The control of such joints imposes difficulties as a control torque cannot be applied to assist in the direction of motion and it must constantly satisfy (5).

The presented $(n+1)$-degrees of freedom system can be decoupled to two sub-systems. The first sub-system is the object's model similar to a simple pendulum. We give this object model the term *Object-Pendulum Model* (OPM). However, the OPM's pivot has a control input of normal force f_N that exerts friction torque and a control input for the acceleration $\mathbf{a}$ generated at pivot e by the arm. Acceleration $\mathbf{a}$ is given by

$$\mathbf{a} = J\ddot{\mathbf{q}} + \dot{J}\dot{\mathbf{q}} \tag{6}$$

where J is the Jacobian matrix of the robotic arm mapping the joint's angular velocity to the gripper's linear velocity. The OPM's coordinate frame $\mathcal{O}_p$ is fixed to the pivot with its y_p-axis parallel but opposite to gravity. We measure the OPM's angle ϕ relative to the y_p axis and the positive direction is taken counter-clockwise. In this form, angle ϕ equals the sum of the gripper's pitch angle and the relative angle, that is, $\phi(t) = \psi(t) + \theta(t)$ (Figure 3a). For consistency, angle ϕ is measured such that $|\phi(t)| \leq \pi$. In this configuration, the OPM's equation of motion is given by

$$M\ddot{\phi} - mgl\sin\phi + m(\mathbf{a}\cdot\hat{\mathbf{r}})l = \tau(f_N) \tag{7}$$

where $M = I + ml^2$, $\hat{\mathbf{r}} = (\ -\cos\phi \quad -\sin\phi\ )^T$ is a unit vector perpendicular to the OPM's length and $\tau(f_N)$ is the friction torque according to (4). For simplicity and to mimic the motion of the human arm, while controlling the motion of the OPM's gripper, we constrain the arm to provide acceleration only in the x_p direction. Therefore, the equation of motion of the OPM is

$$M\ddot{\phi} - mgl\sin\phi - mal\cos\phi = \tau(f_N) \tag{8}$$

where a is the acceleration intensity in the horizontal direction. Further, let $\mathbf{x} = (x_1 \quad x_2)^T$ be the state of the system where $x_1 = \phi$ and $x_2 = \dot{\phi} = \dot{x}_1$. System (8) can be rewritten in the state space form as

$$\dot{\mathbf{x}} = \mathbf{f}(\mathbf{x},\mathbf{u}) = \begin{pmatrix} x_2 \\ M^{-1}(\tau + mgl\sin x_1 + mal\cos x_1) \end{pmatrix} \tag{9}$$

where $\mathbf{u} = (\tau \quad a)^T$. Note that although system $\mathbf{f}(\mathbf{x},\mathbf{u})$ has two inputs and a one degree of freedom system needs only one for stabilization, the linearization point is not an equilibrium. Therefore, input a cannot stabilize the system by its own nor the semi-active joint τ, which has a dissipative property.

The second sub-system is the robotic arm given in (1). The arm has two roles. Its first role is to provide the acceleration $\mathbf{a}$ at the pivot point of the OPM to control its angle ϕ. The second role is to apply, using the arm's gripper, normal force f_N at the pivot point to enable or disable relative motion between the OPM and the gripper. In this work we focus on the control of the OPM using f_N and a. Nevertheless, the

control of the robot to provide acceleration a is well known [28] and is not in the scope of this paper.

B. Problem Definition

The regrasping problem is defined as follows. Object $\mathcal{B}$ is held by the gripper of system (1) as described in section II-A. Given the initial angle $\theta(t=0)=\theta_o$ between object $\mathcal{B}$ and the gripper, perform some manipulation motion such that

$$\lim_{t\to\infty}\theta(t)=\theta_d\ ,\quad \lim_{t\to\infty}\dot{\theta}(t)=0. \tag{10}$$

In other words, the manipulation motion should bring the object to relative angle θ_d with zero velocity. In terms of the OPM configuration, with constant pitch angle ψ easily set by the manipulator, the initial OPM angle is $\phi_o=\theta_o+\psi$. Hence, the goal in terms of the OPM angle would be

$$\lim_{t\to\infty}\mathbf{x}(t)=\mathbf{x_d} \tag{11}$$

where $\mathbf{x_d}=(\theta_d+\psi_d\ \ 0)^T=(\phi_d\ \ 0)^T$.
Several assumptions are made in this work:

- It is assumed that the state (angles and angular velocities) of the OPM and robot are fully known. That is, feedback of the angles $\mathbf{q}$ and θ is acquired at all times, as well as their angular velocities $\dot{\mathbf{q}}$ and $\dot{\theta}$. This state feedback can be acquired by cameras or motion capture systems. However, sensing and estimation are beyond the scope of the paper.
- The properties I, m, l, L of object $\mathcal{B}$ are assumed to be fully known.
- The joints' torques of the robotic arm are not limited and can supply any desired gripper acceleration. Torque saturation is beyond the scope of this paper.

C. Gripper Holding Force

The minimal normal force required to hold the object in the gripper without linear slippage due to inertial force is calculated next. Let ω_{gp} and α_{gp} be the gripper's angular velocity and acceleration vectors, respectively. The angular velocity vector ω_l and acceleration vector $\dot{\omega}_l$ of the OPM are given according to the Newton-Euler method [29]

$$\omega_l=\omega_{gp}+\dot{\phi}\mathbf{z_l} \tag{12}$$

$$\dot{\omega}_l=\dot{\omega}_{gp}+\ddot{\phi}\mathbf{z_l}+\omega_{gp}\times(\dot{\phi}\mathbf{z_l}) \tag{13}$$

where $\mathbf{z_l}$ is the rotation axis vector of $\mathcal{B}$ about the pivot point e calculated according to the robot's direct kinematics. By application of the Newton-Euler method [30], the linear acceleration of the OPM's COM is

$$\dot{\mathbf{v}}_\mathbf{l}=\dot{\mathbf{v}}_\mathbf{gp}+\dot{\omega}_l\times\mathbf{l}+\omega_l\times(\omega_l\times\mathbf{l}) \tag{14}$$

where $\mathbf{l}$ is the vector from pivot e to the OPM's COM represented in the $\mathcal{O}$ frame and $\mathbf{v_{gp}}$ is the gripper's linear velocity vector. Consequently, the inertial forces acting on the OPM's COM are given by

$$\mathbf{F_l}=m\dot{\mathbf{v}}_\mathbf{l}. \tag{15}$$

Note that the expression in (15) contains terms of $\ddot{\phi}$ and $\ddot{\mathbf{q}}$ that are difficult to measure. Thus, they are calculated based on the models (8) and (1), respectively. However, we are interested in the forces acting on the OPM's motion plane. In particular, we compute the radial force f_r acting along the OPM and the tangential force f_t acting perpendicular to the OPM (Figure 3b). Both are calculated by

$$f_r=\mathbf{F_l}\cdot\hat{\mathbf{l}}\ ,\qquad f_t=\mathbf{F_l}\cdot\hat{\mathbf{r}} \tag{16}$$

where $\hat{\mathbf{l}}$ is a unit vector in direction of $\mathbf{l}$.

From (16), the net force that must be resisted at the pivot is $f=\sqrt{f_r^2+f_t^2}$. Therefore, the normal force exerted by the gripper must satisfy $|f|\le\mu f_N$ where μ is the linear coefficient of friction. During swinging of the OPM, we set the normal force to be as minimal as possible with a user-defined safety factor $\alpha>1$, that is,

$$f_N=\frac{\alpha}{\mu}f=\frac{\alpha}{\mu}\sqrt{f_r^2+f_t^2}. \tag{17}$$

The safety factor α is used to keep the normal force above the minimal value in case of small disturbances. In such a case, there will be no linear slippage. In this work we assume that the inertial forces (16) developed on the OPM are not that large such that the resulted normal force f_N from (17) is able to prevent linear slippage but will not cause angular sticking. This assumption is validated in the simulation sections.

III. Swing-up Regrasping Motion

In the proposed motion, the OPM is swung-up above the desired angle from where the motion is toward the desired state with the assistance of gravity. The motion is divided into two phases. The first phase is the *Swing-Up* phase where the OPM is provided with enough energy to reach the Region-of-Attraction (ROA) of the desired final state $\mathbf{x_d}$. The definition of the ROA will be given further on. The swing-up phase is based on an Impulse-Momentum approach where the system is given enough energy to reach above the height of the goal state. Once the OPM is in the ROA, at some time t_c the second phase termed *Gravity-Assisted Stabilization* (GAS) is initiated, aimed to stabilize the OPM in its goal state. A limited Linear Quadratic Regulator (LQR) controller termed *Clipped LQR* (cLQR) is used based on the properties of the semi-active joint of the pivot.

In this section, we will present the cLQR controller for the GAS phase and discuss the terms of its operation. Note that after the swing-up phase brings the OPM to the ROA at time t_c, the robotic arm stops and remains stationary. Hence, the acceleration input is set to $a(t>t_c)=0$ and the pitch $\psi(t>t_c)=\psi_d=Const.$ remains constant. Therefore, in

this GAS phase, we assume zero motion of the robotic arm apart from the OPM and the closing/opening gripper. Further, the ROA is defined based on such a controller to further understand what is expected of the swing-up phase presented later on. We begin by discussing the GAS phase, which will define the needs for the first phase.

A. LQR control of a fully actuated pendulum

We first examine the stabilization of a fully actuated pendulum, that is, with an actuator not constrained to the dissipation constraint (5). Consider the system in (9) with $a = 0$. We wish to stabilize the system on $\mathbf{x_d}$. Further, the desired torque τ_d to hold the OPM stationary at $\mathbf{x_d}$ must satisfy $\mathbf{f}(\mathbf{x}, \tau_d) = 0$, which yields the gravity resisting torque $\tau_d = -mgl \sin x_1$. Therefore, we define the error state $\mathbf{x_e} = \mathbf{x} - \mathbf{x_d}$ and the input error $\tau_e = \tau - \tau_d$. Linearization of the system around $(\mathbf{x_d}, \tau_d)$ yields the linear time-invariant continuous-time system

$$\dot{\mathbf{x}}_\mathbf{e}(t) = A\mathbf{x_e}(t) + B\tau_e(t) \tag{18}$$

where

$$A = \begin{bmatrix} 0 & 1 \\ M^{-1}mgl\cos\phi_d & 0 \end{bmatrix}, \quad B = \begin{pmatrix} 0 \\ M^{-1} \end{pmatrix} \quad , \tag{19}$$

and $\mathbf{x_e}(t_c) = \mathbf{x}(t_c) - \mathbf{x_d}$ is the initial condition. We define a quadratic cost function of the form

$$J(\mathbf{x_e}) = \int_{t_c}^{\infty} \left(\mathbf{x_e}^T Q \mathbf{x_e} + R\tau^2 \right) dt \tag{20}$$

with $Q = Q^T \geq 0$ and $R > 0$ as positive definite weighting matrices that provide an optimal feedback control [31]

$$\tau_e^* = -R^{-1}B^T P\mathbf{x_e} = -K\mathbf{x_e} \;\Rightarrow K = -R^{-1}B^T P \tag{21}$$

where P is the solution of the Riccati equation

$$Q - PBR^{-1}B^T P + PA + A^T P = 0 \; . \tag{22}$$

The cost-to-go of the optimal control policy is

$$J^*(\mathbf{x_e}) = \mathbf{x_e}^T P \mathbf{x_e} \; . \tag{23}$$

From (21), the feedback control that would be applied to (9) (or (8)) would be

$$\tau^* = -K(\mathbf{x} - \mathbf{x_d}) + \tau_d \; . \tag{24}$$

The control law in (24) could provide torque in both clockwise and counter-clockwise directions, without taking into account the dissipative constraint in (5). Torques that do not satisfy (5) demand negative normal force from the gripper, a demand that cannot be satisfied. Therefore, attention must be paid and the controller should be modified to force $f_N \geq 0$. In this case, the control signal from (24) is clipped, and the modified controller is termed *Clipped* LQR (cLQR) [22], [24]. However, a distinction must be made between two different motions. The first kind is when the motion at $t > t_c$ is toward the desired state with the assistance of gravity. This happens when the conditions

$$|\phi| < |\phi_d| \text{ and } \left(sgn(\dot{\phi}) = sgn\left(mgl\sin\phi\right) \text{ or } \dot{\phi} = 0 \right) \tag{25}$$

are satisfied. The second kind is when the OPM moves toward the goal but encounters resistance from gravity. This happens when

$$|\phi| > |\phi_d| \quad \text{and} \quad sgn(\dot{\phi}) \neq sgn\left(mgl\sin\phi\right). \tag{26}$$

In such motion, the OPM will swing toward the goal against gravity and be caught at the desired angle, preferably with zero velocity. An energy control based approach for such motion proposed in [32]. This kind of motion is not considered in this paper and we deal with the first kind. Next, we propose the cLQR controller to stabilize the OPM.

B. Clipped LQR stabilization

The GAS phase is characterized by motion toward the goal while the angular velocity has the same direction as the gravity torque acting on the OPM (Condition (25)). Let regions I and II in Figure 4 be the regions above the goal angle and in the left half-plane. They are considered united for now, while a distinction between them would be given later on. Consider a simple case where the OPM is located in region I or II with zero or positive velocity (counter-clockwise toward the goal ϕ_d). In such case, a fully actuated OPM with control law (24) would have one of the control torque τ^* profiles shown in Figure 5. The exact profile will be determined by the initial state $\mathbf{x}(t_c)$ at the time of initiating the controller. Some of the profiles begin with positive torque and converge to the negative steady-state holding torque τ_d. In such cases, the optimal control applies positive torque, in the direction of velocity, to accelerate and assist the motion just before applying negative torque for deceleration and braking at the goal angle. However, a semi-active joint with model (4) could not perform such transition as it cannot apply negative normal force at the contacts. Recall that in this case the velocity is positive and according to the dissipative constraint in (5), the friction torque can only be negative. In this case, implementing a Constrained LQR controller [33], [34] is possible. However, such a controller is more complex to apply and we seek for a much simpler controller. Hence, we clip the above LQR control to apply only negative torque, that is, only positive normal force.

The pivot of the OPM function as a semi-active joint and the LQR controller can only supply negative torque by applying positive normal force. To solve this, we can take advantage of gravity for assistance when the optimal control torque is positive. Thus, the aim of the swing-up phase will be to bring the OPM to region I or II as shown in Figure 4 with zero or positive velocity. However, if region I is reached with

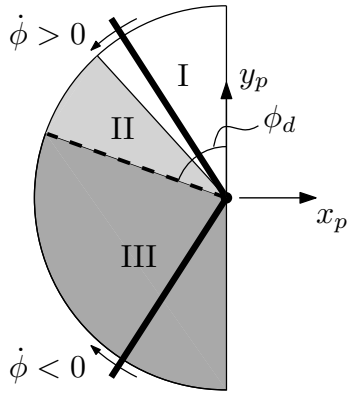

Fig. 4. Motion regions.

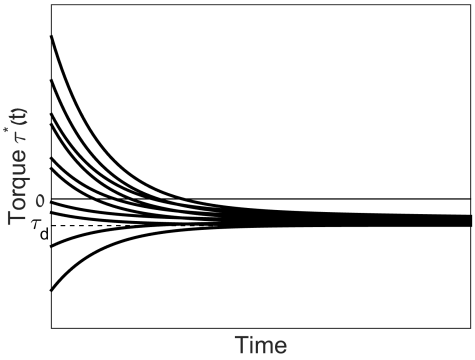

Fig. 5. Torque input for a fully actuated OPM in GA motion.

zero or positive velocity, the OPM will be allowed to swing-down freely until it reaches the ROA of the LQR, that is, region II. Note that in the swing-down, the normal force will be defined to resist inertial forces as defined in (17). Region II is termed GAS-ROA and is defined to be the region where the optimal torque is $\tau^* < 0$. The expression for τ^* is linear and the condition for entering the GAS-ROA is therefore given according to (24) by

$$\tau^* < 0 \Rightarrow x_2 > \frac{1}{k_2}(\tau_d - k_1(x_1 - \phi_d)) \tag{27}$$

If the swing-up manipulation brings the OPM directly to the GAS-ROA, satisfying (27), τ^* is initiated there without free swing-down. In summary, the cLQR is initiated at time t_c when (25) is satisfied and it defines the control normal force by

$$f_N(t > t_c) = \begin{cases} \frac{1}{\nu}|\tau^*|, & x_2 > \frac{1}{k_2}(\tau_d - k_1(x_1 - \phi_d)) \\ \frac{1}{\mu}\sqrt{f_r^2 + f_t^2}, & \text{otherwise} \end{cases} \tag{28}$$

Next, we refer to the swing-up phase using a method based on impulsive-momentum approach to bring the OPM to the region I or II above the goal.

C. Impulse based Swing-up

The purpose of the swing-up phase is to bring the OPM above the desired goal angle ϕ_d to ϕ_{su}, where $0 < \phi_{su} < \phi_d$ (the choice for ϕ_{su} will be discussed later on) and from where the cLQR will be initiated. For that matter we use an Impulse-Momentum approach inspired by [19]. The stages of the manipulation in the left half-plane are organized in Table I. Specific values and notations in the table would be defined in the proof of Theorem 1 bellow. At time $t = 0$ (stage 0), the object and arm are stationary at their initial pose. In the Impulse-Momentum approach, we first apply an initial impulse force (stage 1) at the pivot to grant the OPM with initial velocity and increase its energy. After impulse, the OPM will move away from the goal (stage 2) with positive angular velocity until reaching momentary stop and direction change. In this stage, the gripper is moved along with the pivot in a constant velocity to preserve the OPM's energy while the object swings toward the goal. We avoid changing the grippers velocity at this stage as it would result in undesired increase or decrease of kinetic energy. Then, at the right angle (to be defined), the gripper is suddenly stopped (stage 3), an event which causes a change in momentum and increases the OPM's energy to the desired level. Therefore, the OPM will swing toward ϕ_{su} (stage 4). Once the OPM passes the goal angle ϕ_d and changes its direction again, the cLQR is initialized (stages 5-6). To simplify our calculations, the swing-up is done along the x-axis. Moreover, we maintain constant pitch angle of the gripper, which eliminates its angular velocity from the equations. Next is the energy analysis to determine the initial impulse force that will elevate the OPM to angle ϕ_{su}.

An impulse force applied at the pivot of the OPM will result in change of its linear and angular momentum. The following Theorem defines the magnitude of the impulse force F_{imp} to gain the OPM with the desired energy to reach ϕ_{su}.

Theorem 1. *Let $\Delta E_d = E_d^{su} - E_0$ be the desired energy gain for the swing-up where $E_0 = mgl(\cos\phi_0 + 1)$ is the OPM's energy at the initial state $\mathbf{x_0}$, and $E_d^{su} = mgl(\cos\phi_{su} + 1)$ is the desired energy of the goal angle ϕ_{su} with zero velocity. The required impulse force F_{imp} applied at the pivot point for time interval Δt_1 to gain energy ΔE_d is*

$$F_{imp} = \mp\frac{\sqrt{2M}}{\Delta t_1 l(\cos^2\phi_0 - 1)}\left(\sqrt{\Delta E_d + mgl(\cos\phi_0 + 1)}\right. \\ \left. \pm\sqrt{\Delta E_d\cos^2\phi_0 + mgl(\cos\phi_0 + 1)}\right). \tag{29}$$

Proof: An impulsive force $\mathbf{F_{imp}} = (F_{imp} \quad 0 \quad 0)^T$ is applied in the x direction, which causes angular momentum change according to

$$-\mathbf{l} \times \mathbf{F_{imp}}\Delta t_1 = M(\dot{\phi}_1 - \dot{\phi}_0) \tag{30}$$

where $\mathbf{l} = l(-\sin\phi_0 \quad \cos\phi_0 \quad 0)^T$ is the vector from the

TABLE I
STAGES OF THE IMPULSE BASED SWING-UP MANIPULATION.

Index	Stage	Time	Angle	OPM vel.	Pivot acc.	En. gain
0	Initial pose	$t = 0$	$\phi = \phi_0$	$\dot{\phi} = 0$	$a = 0$	0
1	Impulse	$t \leq \Delta t_1$	$\phi > \phi_0$	$\dot{\phi} > 0$	$a < 0$	ΔE_1
2	Const. pivot vel.	$\Delta t_1 < t < t_2$	$\phi > \pi$	$\dot{\phi} \geq 0 \Rightarrow \dot{\phi} < 0$	$a = 0$	0
3	Pivot brake	$t_2 \leq t < t_3$ $t_3 = t_2 + \Delta t_{23}$	$\phi = \pi$	$\dot{\phi} < 0$	$a > 0$	ΔE_2
4	Swing-up	$t > t_3$	$\phi_{su} < \phi < \pi$	$\dot{\phi} < 0$	$a = 0$	≈ 0
5	Initiate cLQR	$t = t_4$	$\phi \approx \phi_{su}$	$\dot{\phi} = 0$	$a = 0$	0
6	At goal angle	$t = t_5$	$\phi = \phi_d$	$\dot{\phi} = 0$	$a = 0$	-ΔE

pivot to the COM, $\Delta t_1 << 1$ is a short time interval where the impulsive force acts, $\dot{\phi}_0 = 0$ and $\dot{\phi}_1$ are the angular velocities before and after the impulse force acts. Solution of (30) provides the generated velocity after impulse

$$\dot{\phi}_1 = \frac{1}{M} F_{imp} l \cos\phi_0 \Delta t_1 \ . \tag{31}$$

Moreover, the impulsive force generates linear velocity in the x direction given by

$$F_{imp}\Delta t_1 = m v_c \ \Rightarrow \ v_c = \frac{1}{m} F_{imp}\Delta t_1 \ . \tag{32}$$

During the short time interval Δt_1, the OPM's angle has not changed, $\phi_0 = \phi_1$, and therefore no change in potential energy occurred. Hence, the impulsive force caused only change in the kinetic energy:

$$\Delta E_1 = \frac{1}{2} M \dot{\phi}_1^2 + \frac{1}{2} m \mathbf{v_c}^T \mathbf{v_c} - \frac{1}{2} M \dot{\phi}_0^2 \tag{33}$$

where the last component is equal to zero by the initial state definition. Note that there is no energy loss due to friction as there is no angular change.

Due to the impulsive force, the OPM will rotate counter to the goal. The gripper now must maintain constant linear velocity $\mathbf{v_c} = (v_c \ \ 0 \ \ 0)^T$ to allow the OPM to momentarily stop and revert its direction toward the goal without additional energy change. After the OPM has reversed its direction due to gravity, a sudden brake of the gripper, while it is swinging toward the goal, is performed. This sudden brake would increase the energy of the swinging object and enable it to reach the goal. If the brake occurs before direction change, sudden braking will cause energy decay instead of the desired increase. Such sudden braking is performed using the control law for the arm's joints

$$\ddot{\mathbf{q}} = -W\dot{\mathbf{q}} \tag{34}$$

where W is a diagonal matrix of positive gains controlling the exponential decay of $\dot{\mathbf{q}}$. Large gains in W would cause sudden braking of the gripper in a very short time interval Δt_{23}. Moreover, it would cause an impulsive force $\mathbf{F_b}$ and moment $\mathbf{M_b}$ on the OPM. The impulsive force and moment would result in sudden change in the linear and angular momentum of the OPM, respectively, given by

$$\mathbf{F_b}\Delta t_{23} = m(\mathbf{v_3} - \mathbf{v_2}) \tag{35}$$

$$\mathbf{M_b}\Delta t_{23} = -\mathbf{l} \times \mathbf{F_b}\Delta t_{23} = M(\dot{\phi}_3 - \dot{\phi}_2) \tag{36}$$

where $\dot{\phi}_2$ and $\dot{\phi}_3$ are the angular velocities before and after the sudden braking, respectively. $\mathbf{v_2}$ and $\mathbf{v_3}$ are the linear velocities of the OPM's COM before and after the braking and are expressed by

$$\mathbf{v_2} = -\dot{\phi}_2 l \begin{pmatrix} \cos\phi_2 \\ \sin\phi_2 \\ 0 \end{pmatrix} + \mathbf{v_c}, \quad \mathbf{v_3} = -\dot{\phi}_3 l \begin{pmatrix} \cos\phi_2 \\ \sin\phi_2 \\ 0 \end{pmatrix} . \tag{37}$$

By substituting (35) in (36) and using (37), we acquire

$$\dot{\phi}_3 = \dot{\phi}_2 + \frac{1}{M} m l v_c \cos\phi_2 \tag{38}$$

From (38) we can easily see that braking at angle

$$\phi_2 = \begin{cases} 0, & \dot{\phi}_2 > 0 \\ \pi, & \dot{\phi}_2 < 0 \end{cases} \tag{39}$$

will result in maximum angular velocity and kinetic energy increase. Without loss of generality, as we work on the left half-plane, we take $\phi_2 = \pi$. Braking at that angle will result in lower demand for initial impulse force F_{imp}. Therefore, we define the brake to occur once the OPM points downwards, that is, once $\phi_2 = \pi$. This, along with (32) yields

$$\dot{\phi}_3 = \dot{\phi}_2 - \frac{F_{imp} l \Delta t_1}{M} \ . \tag{40}$$

Here also, no angular change is made during the brake time and therefore there is no change in potential energy, and no energy loss due to friction. Therefore, the kinetic energy change due to the sudden braking is

$$\Delta E_2 = \frac{1}{2} M \dot{\phi}_3^2 - \frac{1}{2} M \dot{\phi}_2^2 - \frac{1}{2} m \mathbf{v_c}^T \mathbf{v_c} \ . \tag{41}$$

Conservation of energy from $t = \Delta t_1$ just after the first impulse to $t = t_2$ right before the brake provides us with

the equality

$$\frac{1}{2}M\dot{\phi}_1^2+\frac{1}{2}m{\mathbf{v_c}}^T\mathbf{v_c}+mgl(\cos\phi_1+1)-\int_{\phi_1}^{\phi_2}\tau d\phi=\frac{1}{2}M\dot{\phi}_2^2+\frac{1}{2}m{\mathbf{v_c}}^T\mathbf{v_c}+mgl(\cos\phi_2+1) \quad (42)$$

where $\tau=\tau(\phi)$ is the torsional friction at the pivot point. From (42) and with $\phi_2=\pi$ we acquire

$$\dot{\phi}_2=\sqrt{\dot{\phi}_1^2+\frac{2mgl}{M}(\cos\phi_0+1)-\int_{\phi_1}^{\phi_2}\tau d\phi} \quad (43)$$

The total energy change gained by the impulse force and sudden braking is $\Delta E=\Delta E_1+\Delta E_2$. Therefore, using (31),(33), (40)-(43) we acquire

$$\Delta E=\frac{1}{2}M\left(\dot{\phi}_2+\frac{F_{imp}l\Delta t_1}{M}\right)^2-mgl(\cos\phi_0+1)-\int_{\phi_0}^{\phi_2}\tau d\phi \quad (44)$$

with $\dot{\phi}_2$ given by (43). The integral component, which expresses the energy loss due to friction, can be neglected as we do not aim to reach exactly to $\mathbf{x_d}$ but somewhere above it. Later in the simulations we will show that this assumption is feasible.

Demanding that ΔE of (44) will be equal to the desired energy increase ΔE_d and solving for F_{imp} yields two solutions given in (29). The solution that will provide force in the desired direction (negative in our left half-plane case) will be chosen. Note that ϕ_0 cannot be equal to 0 or π as it will cause the denominator of the first term in (29) to be zero and would demand a non-physical impulse force. ■

Theorem 1 provides us with the essential impulsive force F_{imp} to increase the OPM's energy above the desired angle. Once it reaches this level, the cLQR can be initialized. As mentioned, the impulse force F_{imp} does not take the energy loss due to friction into consideration. That is, in a frictionless system this force will bring the OPM exactly to the desired angle. However, as described in Section II-C, the gripper applies force to maintain friction in order to prevent linear slippage of the pivot. Hence, energy loss exists. Nevertheless, the swing-up phase aims to bring the OPM above the desired angle ϕ_d. Thus, in theory we can set the swing-up goal angle $\phi_{su}=\theta_{su}+\psi$ anywhere above ϕ_d. But this should be done carefully as an angle close to ϕ_d might not be reached due to the friction loss. And an angle too large might reach over the upright angle $\phi=0$ and diverge to the other side. Therefore, we set the swing-up angle to be at the middle such that $\phi_{su}=\frac{\phi_d}{2}$. Moreover, ϕ_d must be large enough for ϕ_{su} to be far enough from these boundaries. Thus, the pitch angle ψ must be chosen such that

$$|\phi_d|>\xi \quad (45)$$

where $\xi>0$ is a user-defined value. As we decrease ξ, the required additional energy $E_d^{su}-E_d$ to reach above the desired angle to ϕ_{su} decreases as well. Thus, there is a minimum limit where beneath it the frictional loss exceeds this additional energy and the OPM would not even reach ϕ_d. In the simulation section we propose a suitable value for ξ.

The selection of the pitch angle should minimize the impulse force F_{imp} required for swing-up to ϕ_{su}. Minimization of F_{imp} is essential to achieve low gripper accelerations and joint torques, and reduce the risk of linear slippage. By assuming that the pitch angle at the left half-plane side case is limited to $0\leq\psi\leq\pi$, Figure 6 presents the impulse force given by (29) with regard to the pitch angle for several initial angles. It can be seen that the minimum impulse force is acquired near the pitch boundaries. Thus, the minimization would select an impulse force as close as possible to these boundaries based on the following optimization problem:

$$\begin{aligned}&\underset{\psi}{\text{minimize}} && |F_{imp}|\\ &\text{subject to} && (1)\ \phi_0=\theta_0+\psi\neq 0\\ &&& (2)\ \phi_0=\theta_0+\psi\neq\pi\\ &&& (3)\ |\theta_d+\psi|>\xi \text{ (from (45))}\\ &&& (4)\ \text{Arms kinematic and dynamic constraints.}\end{aligned}$$

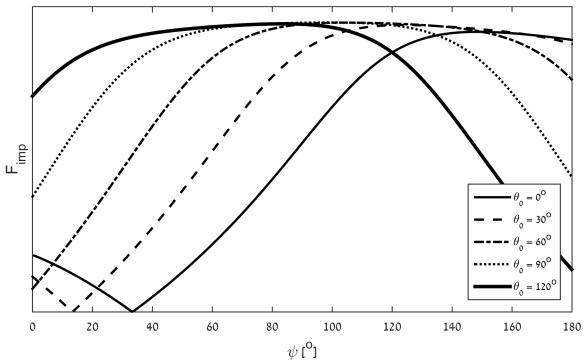

Fig. 6. Impulse force with regard to the pitch angle for several initial angles θ_0.

The above optimization problem minimizes the impulse force to find the optimal pitch angle subject to several constraints. First, a pitch angle that causes $\phi_0=\theta_0+\psi=0$ or $\phi_0=\pi$ should be avoided to prevent an excessively large impulse force. Second, criterion (45) must be enforced to ensure swing-up above the desired angle. Last, the kinematic and dynamic constraints of the arm define a feasible range for the pitch angle. However, because the arm's motion planning is not considered in this paper, we leave the choice for ψ as user-defined and engage this problem in future work.

IV. Simulations and Experiments

In this section we present simulations and experiments conducted to validate the proposed swing-up regrasping approach. However, to use feasible and realistic torsional friction coefficients in the simulations and experiments, appropriate measurements were conducted and are first presented.

A. Friction coefficients measurements

Before performing simulations and experiments to validate the proposed method, feasible frictional coefficients are required for the model. However, we did not find documentation in literature for torsional friction values. Moreover, we need to select feasible coefficients that will provide high tangent friction but rather low torsional friction, a property that will require relatively low normal forces applied to the object. Therefore, measurements were conducted on two 3D printed semi-sphere fingertips made of different materials. The first material was a rubber-like polymer[1] shown on the right of Figure 7a tested on a PVC surface. The second material is a rigid polymer[2] shown left in Figure 7a. This material was designated to slide on an aluminum surface. To measure the frictional coefficients of the materials we performed an experiment. Each fingertip was mounted on a 6-axis ATI Force/Torque transducer (Figure 7b). First, to measure the torsional friction coefficient, the fingertip was twisted against the surface with different normal forces while measuring the torque around the rotational axis. To measure the tangential friction, the tangential forces were measured while sliding the fingertip along the surface with different normal forces. The results for the first material are shown in Figure 8 with a linear fit and a slope yielding a torsional friction coefficient of $\nu = 0.0014$. The tangential friction coefficient for the first material was measured to be $\mu = 0.79$. For the second material, the torsional coefficient was measured to be $\nu = 0.00047$ while the tangential coefficient is $\mu = 0.36$. These are dynamic coefficients measured during sliding of the fingertips.

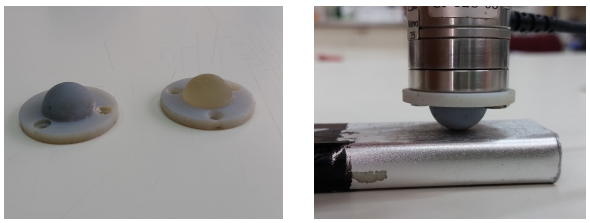

(a) (b)

Fig. 7. (a) Semi-sphere finger-tips used for friction coefficient measurement and the (b) friction measurement between the fingertip and surface with the ATI Nano25 F/T transducer.

[1]PolyJet rubber-like materials supplied by Stratasys®.
[2]Verogray25 DM-8110 supplied by Stratasys®.

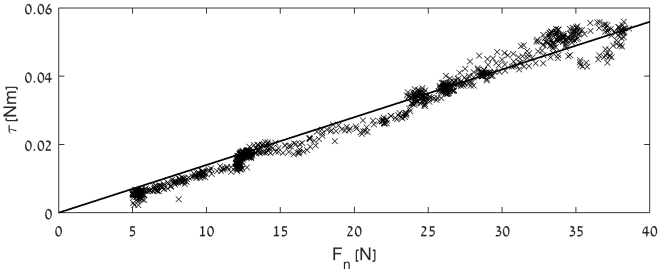

Fig. 8. Torsional friction measurement for the rubber-like material.

B. Simulations

To validate the above method we performed simulations with a six degrees of freedom (DOF) robotic arm. However, due to the planar nature of the method, only three DOF of the arm are needed. The aim of the presented simulation is to regrasp a bottle with the given properties: mass $m = 0.313\ kg$, inertia $I = 1.256 \cdot 10^{-3}\ kg \cdot m^2$, length $L = 0.114\ m$, and COM $l = 0.057\ m$. The bottle is initially grasped at relative angle $\theta_0 = 60^o$ and it is required to regrasp it at angle $\theta_d = -65^o$.

Recall that due to the frictional energy loss, we define a swing-up goal angle ϕ_{su} equal to half of the original goal angle, which is constrained to be $|\phi_d| > \xi$. Based on the measured friction coefficients, simulations have shown that in order to reach above ϕ_d, the limit angle ξ must be at least 40^o. Therefore, we choose the pitch angle to be $\psi = 115^o$, yielding the swing-up goal angle of $\phi_{su} = 25^o$. Choosing a small impulse time interval $\Delta t_1 = 0.015\ s$ provides an impulse force of $F_{imp} = -22.8\ N$ applied by the gripper at the pivot point. For the cLQR control we select $Q = diag([1\ 0.1]^T)$ and $R = 1$, resulting in a control gains vector $K = (1.12\ \ 0.32)^T$. In addition, safety factor α used in (17) to calculate the minimum normal force to be applied by the gripper is chosen, in this case, to be 1.

Snapshots of this motion are shown in Figure 9. After applying impulse F_{imp}, while the gripper maintains constant velocity, the bottle will swing towards the arm until it momentarily stops to reverse its swinging direction to swing downwards freely. Once the angle reaches $\phi = 180^o$ at time $t_b = 0.39\ s$, the gripper is instantly braked to increase the OPM's energy. Once the angle crosses ϕ_d and reaches zero velocity at time $t_c = 0.67\ s$, the cLQR is initiated to stabilize the angle at ϕ_d. In this case, the zero velocity is reached after crossing the GAS-ROA line defined by (27). Therefore, the LQR controller (24) is instantly applied to bring the OPM to ϕ_d with zero velocity.

The phase-plane, angle and energy responses are seen in Figures 10, 11 and 12, respectively. Notice that the OPM does not reach ϕ_{su} or its corresponding energy due to the frictional loss between the impulse and the braking. The acceleration and normal force inputs are shown in Figures

13a and 13b, respectively. The impulse and brake peaks can be seen in both figures. However, the acceleration is zero after the braking because the gripper is stationary and the normal force converges to the force required to hold the OPM at the desired angle $\frac{1}{\nu}|\tau_d|$.

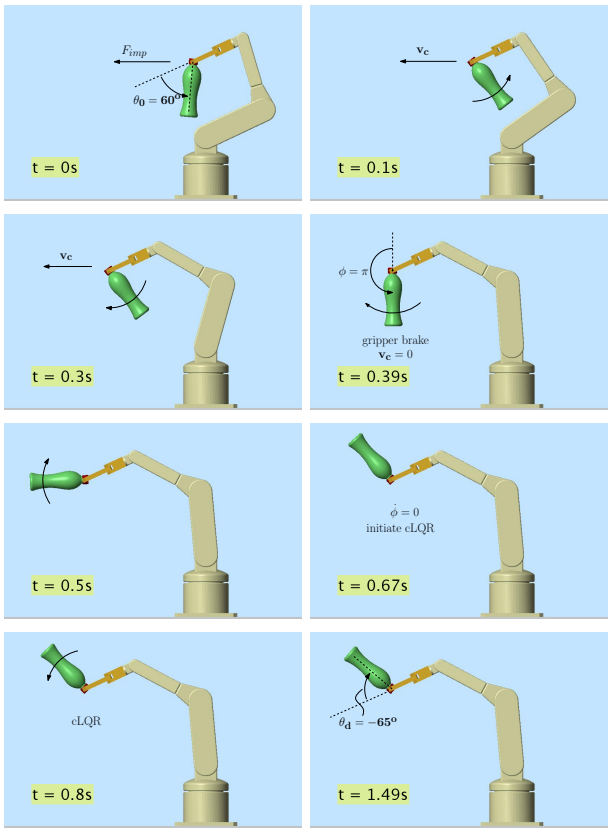

Fig. 9. Simulation of the swing-up motion from $\theta_0 = 60^o$ to $\theta_d = -65^o$.

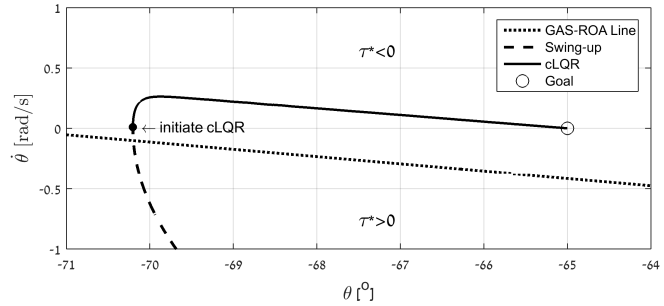

Fig. 10. Phase plane diagram of the swing-up motion around the goal state.

Snapshots of another example of the the swing-up motion can be seen in Figure 14. Here the goal is to regrasp the bottle from angle $\theta_o = 45^o$ to $\theta_d = -140^o$. The angle response can be seen in Figure 15. In this case, the cLQR is initiated at time $t_c = 0.74\ s$ only when it reaches ϕ_{su}. However, this

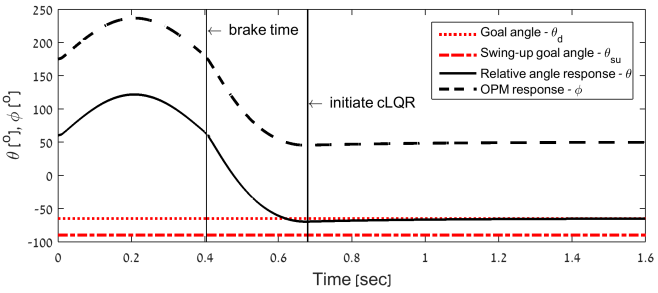

Fig. 11. The OPM's angle response wto regrasp from $\theta_0 = 60^o$ to $\theta_d = -65^o$. The solid curve indicates the angle relative to the gripper while the dashed curve is the angle relative to the vertical.

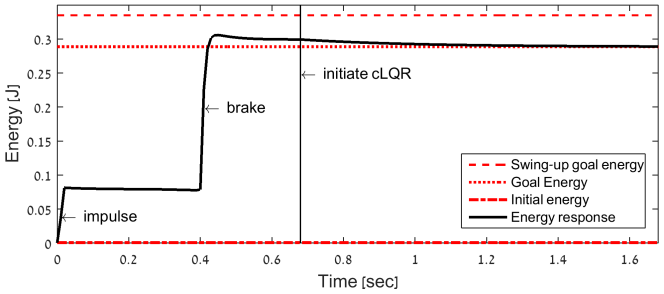

Fig. 12. The OPM's energy response during swing-up regrasping.

is not essential. Once the bottle passes the $\phi = 0$ at time $t = 0.69\ s$, condition (25) is satisfied and controller (28) could then be initiated. The phase-plane diagram around the goal angle can be seen in Figure 16. Note that in this case, the cLQR is initiated at the right half-plane and therefore we require $\tau^* > 0$.

C. Experiments

To validate the impulse based swing-up method proposed with the notion of a semi-active joint controlled by normal force and the cLQR approach, we have designed a swinging rod experiment. We used the 6-DOF Robotis Manipulator-H composed of six Dynamixel-Pro actuators. In addition, a two-jaw gripper was built as seen in Figure 17. The gripper was built using two parallel MX-106R Dynamixel actuators (also by Robotis). These actuators were chosen due to their ability to receive torque commands and therefore apply the desired normal forces on the swinging object. Both the arm and gripper were controlled using Robot Operating System (ROS).

Each jaw of the gripper is composed of a metal plate and a 3D-printed fingertip mounted at its distal end. To prevent the swinging rod from colliding with the arm, the plates were mounted with an angle of 45^o relative to the actuators. Nonetheless, angle θ is measured relative to link 6 of the arm and not to the plates. In addition, the fingers are fixed such that when the jaws are set parallel to each other, the facets

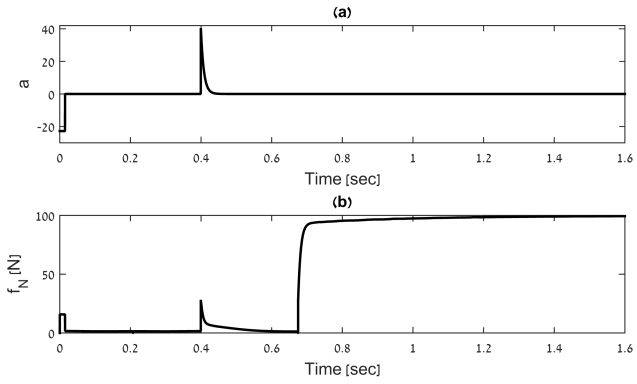

Fig. 13. The inputs to the OPM system: (a) acceleration intensity to the pivot, and (b) the normal force exerted on the OPM by the gripper.

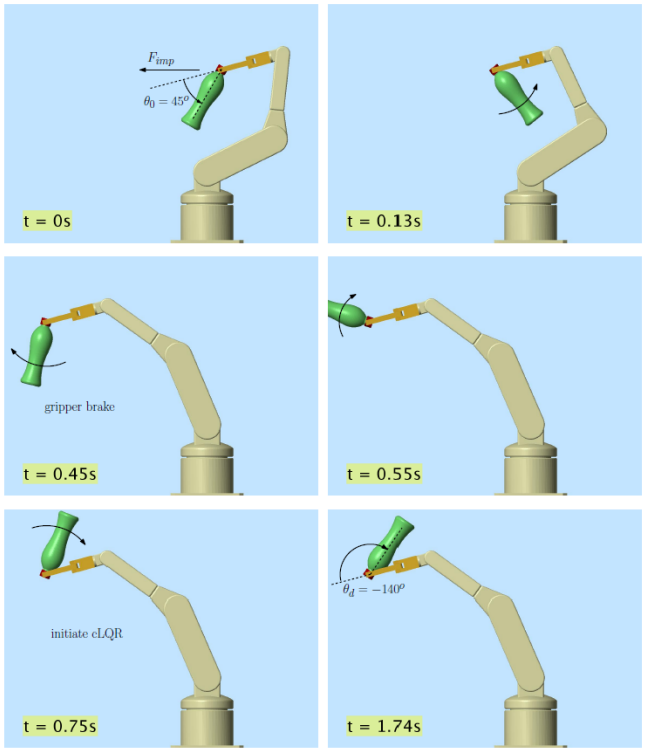

Fig. 14. Simulation of the swing-up motion from $\theta_0 = 45^o$ to $\theta_d = -140^o$.

of the fingers are parallel as well and the distance between them can be varied using screws.

The swinging object was selected to be an aluminum rod with properties: mass $m = 0.028\ kg$, inertia $I = 0.32 \cdot 10^{-3}\ kg \cdot m^2$, length $L = 0.185\ m$, and COM $l = 0.0925\ m$. The coefficients of friction between the printed fingers and rod are the ones measured in Section IV-A: $\nu = 0.00047$ and $\mu = 0.36$. To measure the angle of the rod in real-time, a camera was mounted perpendicular to the plane of motion h. The angle was measured in real-time and the angular velocity

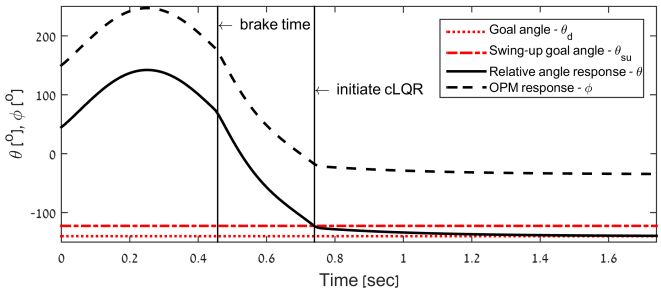

Fig. 15. The OPM's angle response to regrasp from $\theta_0 = 45^o$ to $\theta_d = -140^o$. The solid curve indicates the angle relative to the gripper while the dashed curve is the angle relative to the vertical.

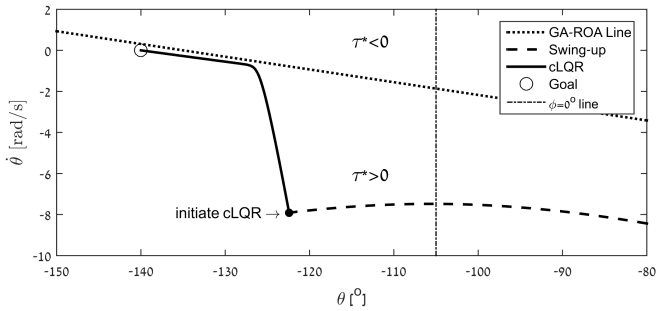

Fig. 16. Phase plane diagram of the regrasp from $\theta_0 = 45^o$ to $\theta_d = -140^o$ around the goal state. Note that the cLQR could already be initiated once the object crosses the $\phi = 0^o$ ($\theta = -105^o$) line from where condition (25) is satisfied.

was calculated by backward finite difference of second order accuracy.

In the presented experiment, the rod was to be regrasped from initial angle $\theta_o = 76.5^o$. The goal angle in this example is chosen to be $\theta_d = 40^o$. Choosing a small impulse

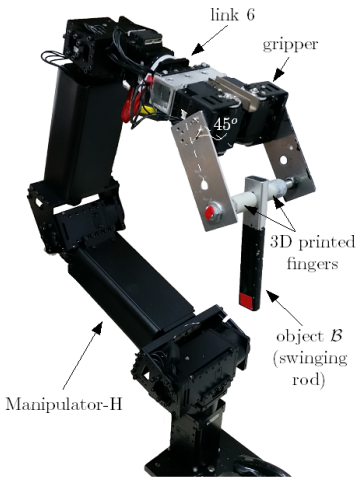

Fig. 17. The experimental setup of a robotic arm, gripper and object to be regrasped through the fingertips semi-active joint.

time interval $\Delta t_1 = 0.01\ s$ provides an impulse force of $F_{imp} = 3.28\ N$ applied by the gripper at the pivot point. The cLQR controller was implemented with $Q = diag([1\ 0.1]^T)$ and $R = 1$ which resulted in the control gains vector $K = (0.86\ \ 0.32)^T$. Note that in the experimental setup, the pitch angle is set to $\psi = 100^o$. The safety factor α to control the minimum normal force to be applied by the gripper is chosen to be 1.3. Snapshots of one test run can be seen in Figure 18 and the angle response is shown in Figure 19. It should be noted that due to noisy signal readings from the camera and dynamixels, a simple mean filter was applied for noise reduction.

In high velocities, the synchronization between the arm's actuators performed poorly and therefore the gripper did not move solely on the x_p-axis. Thus, the gripper's motion along the y_p-axis exerted undesired torques to the rod and reduced its kinetic energy. Nevertheless, the requirement for the swing-up phase to reach above the desired angle compensated for the energy loss and the rod was able to successfully complete the manipulation.

The rod reached near the desired angle at 38.54^o. During the experiments, the grippers actuators were found to exert inaccurate torques. Therefore, the error of 1.46^o or 4% is due to the gripper's inability to accurately provide the desired normal forces to the rod. Nevertheless, such a small error is minor. The results of the experiments validate the approach and show that it is indeed feasible to perform swing-up regrasping using impulse and cLQR control.

V. Conclusions

In this paper we have presented the swing-up regrasping problem and proposed a novel approach to performing it. The approach incorporated a swing-up phase using an impulse-momentum method following a stabilization phase with a cLQR controller to control the semi-active friction joint. In that way the object was swung-up above the goal angle and then brought to the goal in a controlled manner by applying growing normal force. Simulations on a six DOF arm regrasping a bottle were presented to validate the proposed approaches. Moreover, we have shown an experiment fully demonstrating the method.

Future work will involve incorporating the motion planning of the arm for optimization of the pitch angle and the limit angle ξ. Accelerations due to the impulses should be minimized to reduce joint torques. More importantly, estimation methods should be examined to reduce the state feedback dependency and partially approximate the objects state. Moreover, our proposed approach is model based. The human hand does not know in advance the dynamic properties of the manipulated object but manages to approximate them right before performing a successful manipulation. A model identification method or an adaptive control can be applied to approximate the object's dynamic properties in real time.

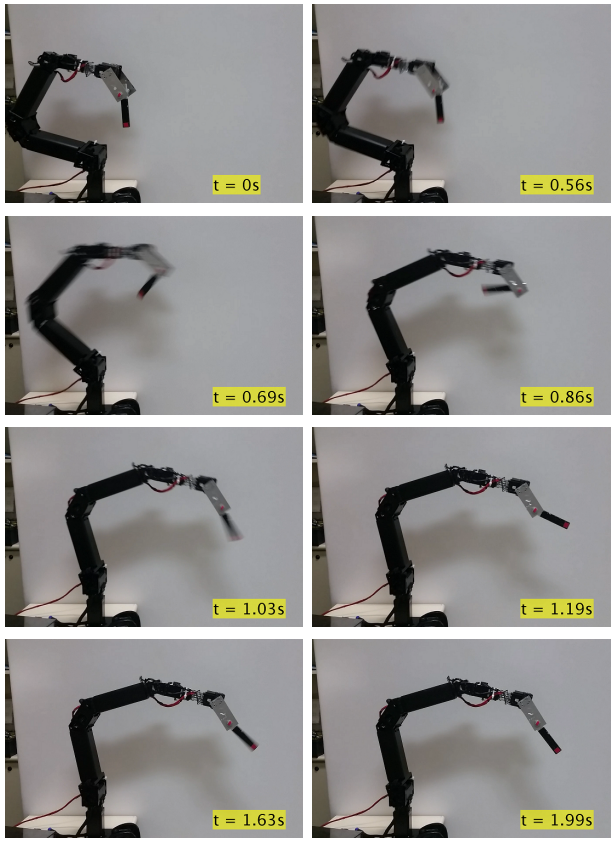

Fig. 18. Snapshots of the experiments. Between times 0s and 1.19s, the object is swung-up from $\theta_o = 76.5^o$ to above the desired angle. Then, the object is controlled by the cLQR and repositioned at $\theta = 38.54^o$ while required to reach $\theta_d = 40^o$.

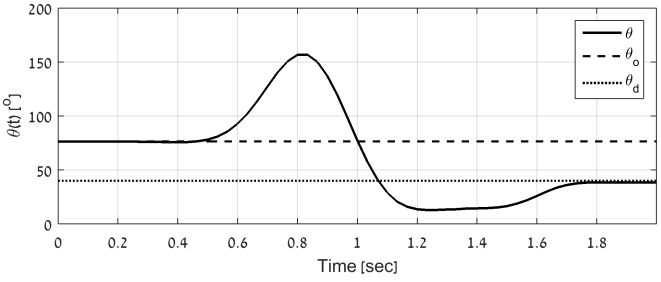

Fig. 19. An experimental result of the rod's angle response.

References

[1] A. A. Cole, P. Hsu, and S. S. Sastry, "Dynamic control of sliding by robot hands for regrasping," *IEEE Transactions on Robotics and Automation*, vol. 8, no. 1, pp. 42–52, Feb 1992.

[2] J.-P. Saut, M. Gharbi, J. Cortes, D. Sidobre, and T. Simeon, "Planning pick-and-place tasks with two-hand regrasping," in *Proceedings of the IEEE/RSJ International Conference on Intelligent Robots and Systems*, Oct 2010, pp. 4528–4533.

[3] P. Tournassoud, T. Lozano-Perez, and E. Mazer, "Regrasping," in *Proceedings of the IEEE International Conference on Robotics and Automation*, vol. 4, 1987, pp. 1924–1928.

[4] B. Corves, T. Mannheim, and M. Riedel, "Re-grasping: Improving

capability for multi-arm-robot-system by dynamic reconfiguration," in *Intelligent Robotics and Applications*. Springer Berlin Heidelberg, 2011, vol. 7101, pp. 132–141.
[5] G. A. de Paula Caurin and L. C. Felicio, "Learning based regrasping applied to an antropomorphic robot hand," ABCM Symposium series in mechatronics, 2006.
[6] M. A. Roa and R. Suarez, "Regrasp planning in the grasp space using independent regions," in *Proceedings of the 2009 IEEE/RSJ international conference on Intelligent robots and systems*, ser. IROS'09, 2009, pp. 1823–1829.
[7] A. Sudsang and T. Phoka, "Regrasp planning for a 4-fingered hand manipulating a polygon," in *Proceedings of the IEEE International Conference on Robotics and Automation*, vol. 2, Sept. 2003, pp. 2671 – 2676 vol.2.
[8] P. Vinayavekhin, S. Kudohf, and K. Ikeuchi, "Towards an automatic robot regrasping movement based on human demonstration using tangle topology," in *Proceedings of the IEEE International Conference on Robotics and Automation (ICRA)*, May 2011, pp. 3332 –3339.
[9] M. Stuheli, G. Caurin, L. Pedro, and R. Siegwart, "Squeezed screw trajectories for smooth regrasping movements of robot fingers," *Journal of the Brazilian Society of Mechanical Sciences and Engineering*, vol. 35, no. 2, pp. 83–92, 2013.
[10] N. Dafle, A. Rodriguez, R. Paolini, B. Tang, S. Srinivasa, M. Erdmann, M. Mason, I. Lundberg, H. Staab, and T. Fuhlbrigge, "Regrasping objects using extrinsic dexterity," in *Proceedings of the International Conference on Robotics and Automation*, May 2014, pp. 2560–2560.
[11] A. Sintov and A. Shapiro, "A computational algorithm for dynamic regrasping using non-dexterous robotic end-effectors," in *Proceedings of the 6th International Conference on Computational Intelligence (IJCCI)*, Rome, Italy, 2014.
[12] N. Furukawa, A. Namiki, S. Taku, and M. Ishikawa, "Dynamic regrasping using a high-speed multifingered hand and a high-speed vision system," in *Proceedings of the IEEE International Conference on Robotics and Automation (ICRA)*, May 2006, pp. 181 –187.
[13] K. Tahara, K. Maruta, A. Kawamura, and M. Yamamoto, "Externally sensorless dynamic regrasping and manipulation by a triple-fingered robotic hand with torsional fingertip joints," in *Proceedings of the IEEE International Conference on Robotics and Automation (ICRA)*, May 2012, pp. 3252 –3257.
[14] L. Consolini and M. Maggiore, "On the swing-up of the pendubot using virtual holonomic constrains," in *Proceedings of the IEEE Conference on Decision and Control*, Dec 2011, pp. 4803–4808.
[15] V. Kurdekar and S. Borkar, "Inverted pendulum control: A brief overview," *International Journal of Modern Engineering Research*, vol. 3, no. 5, pp. 2924–2927, Oct 2013.
[16] I. Fantoni, R. Lozano, and M. Spong, "Energy based control of the pendubot," *IEEE Transactions on Automatic Control*, vol. 45, no. 4, pp. 725–729, Apr 2000.
[17] X. Xin, S. Tanaka, J. hua She, and T. Yamasaki, "Revisiting energy-based swing-up control for the pendubot," in *IEEE International Conference on Control Applications*, Sept 2010, pp. 1576–1581.
[18] K. Astrom and K. Furuta, "Swinging up a pendulum by energy control," *Automatica*, vol. 36, no. 2, pp. 287 – 295, 2000.
[19] T. Albahkali, R. Mukherjee, and T. Das, "Swing-up control of the pendubot: An impulse momentum approach," *IEEE Transactions on Robotics*, vol. 25, no. 4, pp. 975–982, Aug 2009.
[20] R. Jafari, F. Mathis, and R. Mukherjee, "Swing-up control of the acrobot: An impulse-momentum approach," in *American Control Conference (ACC)*, June 2011, pp. 262–267.
[21] J. S. Lane and A. A. Ferri, "Optimal control of a semi-active, frictionally damped joint," in *American Control Conference, 1992*, June 1992, pp. 2754–2759.
[22] P. Dupont, P. Kasturi, and A. Stokes, "Semi-active control of friction dampers," *Journal of Sound and Vibration*, vol. 202, no. 2, pp. 203 – 218, 1997.
[23] H. A. L. Gaul and J. Wirnitzer, "Semi-active friction damping of large space truss structures," *Shock and Vibration*, vol. 11, no. 3-4, p. 173186, 2004.
[24] K. P. Ardeshir Guran, Friedrich Pfeiffer, *Dynamics with Friction: Modeling, Analysis and Experiment*, ser. EBL-Schweitzer. World Scientific Pub., 2001.
[25] R. M. Murray, Z. Li, and S. S. Sastry, *A Mathematical Introduction to Robotic Manipulation*, 1st ed. CRC Press, Mar. 1994.
[26] L. Gaul and R. Nitsche, "The role of friction in mechanical joints," *ASME Applied Mechanics Reviews*, vol. 54, no. 2, pp. 93–106, 2001.
[27] D. Karnopp, "Computer simulation of stick-slip friction in mechanical dynamic systems," *Journal of Dynamic Systems Measurement and Control-transactions of The Asme*, vol. 107, 1985.
[28] A. Bowling and O. Khatib, "Non-redundant robotic manipulator acceleration capability and the actuation efficiency measure," in *Proceedings of the IEEE/RSJ International Conference on Intelligent Robots and Systems*, vol. 4, Oct 2003, pp. 3325–3330.
[29] W. Khalil, "Dynamic modeling of robots using recursive newton-euler techniques," in *ICINCO2010*, Portugal, Jun. 2010.
[30] M. Ardema, *Newton-Euler Dynamics*. Springer, 2005.
[31] R. Tedrake, I. R. Manchester, M. Tobenkin, and J. W. Roberts, "Lqr-trees: Feedback motion planning via sums-of-squares verification," *The International Journal of Robotics Research*, vol. 29, no. 8, pp. 1038–1052, 2010.
[32] A. Sintov and A. Shapiro, "Swing-up regrasping using energy control," in *Proceedings of the IEEE International Conference on Robotics and Automation (ICRA)*, Stockholm, Sweden, 2016.
[33] M. Hassan and E. Boukas, "Constrained linear quadratic regulator: Continuous-time case," *Nonlinear Dynamics and Systems Theory*, vol. 8, no. 1, pp. 35–42, 2008.
[34] A. Kojima and M. Morari, "LQ control for constrained continuous-time systems: an approach based on singular value decomposition," in *Decision and Control, 2001. Proceedings of the 40th IEEE Conference on*, vol. 5, 2001, pp. 4838–4844 vol.5.

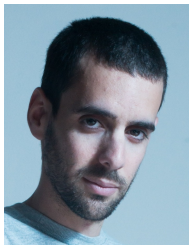

Avishai Sintov received his B.Sc. and M.Sc. degrees in Mechanical Engineering from the Ben-Gurion University of the Negev, Beer Sheva, in 2008 and 2012, respectively. He is currently a Ph.D. student in Ben-Gurion University of the Negev. His interests include grasp planning algorithms, motion planning, dynamic manipulations, climbing robots, and mechanical design.

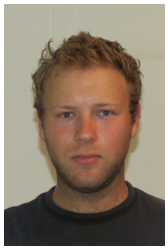

Or Tslil is currently a B.Sc. student in Mechanical Engineering at Ben-Gurion University of the Negev, Beer-Sheva. His interests include robot design, control and programming of robots in ROS and GAZEBO simulator.

Amir Shapiro received the B.Sc., M.Sc., and Ph.D. degrees in Mechanical Engineering from the Technion, Israel Institute of Technology, Haifa, in 1997, 2000, and 2004 respectively. Currently he is an Associate Professor and director of the robotics laboratory at the Department of Mechanical Engineering of Ben-Gurion University of the Negev, Beer-Sheva, Israel. On 2005-2006 he was a post doctoral fellow at the Robotics Institute of Carnegie Mellon University, Pittsburgh, PA. His interests include locomotion of multi-limbed mechanisms in unstructured complex environments, motion planning algorithms for multi-limbed robots, robot grasping-design, control, and stability analysis, robot dynamic manipulations planning, climbing robots, snake like robots, multi-robot on-line motion planning, and agriculture robotics.